

Mechanism of Ferromagnetic Coupling in Copper(II)-Gadolinium(III) Complexes

Jozef Paulovič,[†] Fanica Cimpoesu,^{*,†,||} Marilena Ferbinteanu,[‡] and Kimihiko Hirao^{*,†}

Contribution from the Department of Applied Chemistry, School of Engineering University of Tokyo, Tokyo, Japan 113-8656, and Department of Chemistry, Graduate School of Science, Tokyo Metropolitan University, Tokyo 192-0397, Japan

Received November 17, 2003; Revised Manuscript Received December 29, 2003; E-mail: hirao@qcl.t.u-tokyo.ac.jp; cfanica@qcl.t.u-tokyo.ac.jp

Abstract: This paper offers the first series of state-of-the-art quantum chemical calculations (CASSCF, CASPT2, MS-CASPT2) and analytical models for the well-known problem of quasi-general ferromagnetic coupling in copper–gadolinium complexes. A system chosen from the chemical report of Costes et al. was taken as prototype. At the CASSCF level, calculated results for the experimental structure reproduced the magnetic coupling constant well ($J_{\text{calcd}} = +7.67 \text{ cm}^{-1}$ vs $J_{\text{exp}} = +7.0 \text{ cm}^{-1}$). For more insight, the study molecule was further idealized by geometry optimization to C_{2v} symmetry. Systematic ab initio computation experiments were designed and performed. Owing to specific problems related to the non-*aufbau* ground configuration of the [CuL–Gd] complexes, the calculations were conducted in a nonstandard manner. We found that the qualitative mechanism of Kahn, assigned to the electron jump from 3d of Cu(II) to 5d shell of Gd(III), can be presented effectively as the cause of the phenomenon, if CASPT2 MOs are taken as magnetic orbitals. We showed that the ferromagnetic coupling is also matched and magnified by spin polarization effects over the ligand, in line with the early assumption of Gatteschi. To be distinguished from the initial hypothesis of Gatteschi, which assumed the role of 6s AO of Gd(III), we found that one 5d-type AO is actually involved in the polarization scheme. In fact, the Gatteschi and Kahn mechanisms are not mutually contradictory, but are even interconvertible with appropriate changes of the magnetic orbitals. Within C_{2v} symmetry of complexes, the ferromagnetic coupling can be qualitatively regarded as the preponderant influence of interaction channels exhibiting orbital orthogonality (four 3d–4f contacts) over the nonorthogonal ones (two 3d–4f contacts). The effective preponderance from ferromagnetic pathways is supported by CASPT2 results. One may explain the generality of Cu(II)–Gd(III) ferromagnetic coupling as being correlated with the large occurrence of approximate pseudo- C_{2v} geometry of complexes. The observed orbital regularity is lost in lower symmetries. Thus, the antiferromagnetic exceptions occur when the molecular asymmetry is advanced (e.g., owing to strong chemical nonequivalence of the donor atoms).

I. Introduction

This paper is devoted to the illumination from theoretical and computational modeling perspectives of the celebrated case of quasi-general ferromagnetic coupling between copper(II) and gadolinium(III), encountered in a large number of coordination complexes.¹

Since the first report in 1985,² this general characteristic has been consolidated by a growing amount of experimental evidence,³ to become one of the most pronounced structure–property correlations in molecular magnetism.¹ The widespread occurrence of ferromagnetic coupling in various binuclear and

polynuclear complexes containing Cu(II) and Gd(III) ions, almost irrespective of the ligand nature, is an interesting problem both from a theoretical viewpoint and in terms of its chemical implications. Additionally, the several exceptions that report Cu–Gd complexes with antiferromagnetic interactions⁴ make the problem even more challenging.

Even though frequently stated in the general literature as being a basic magneto-structural correlation,^{1–3} the theoretical explanations have not advanced beyond initial qualitative suggestions. The early interpretation put forward by Gatteschi et al.⁵ proposed spin polarization factors, owing to orbital interaction between

[†] Department of Applied Chemistry, School of Engineering University of Tokyo.

[‡] Tokyo Metropolitan University.

^{||} Permanent address: Institute of Physical Chemistry, Splaiul Independentei 202, Bucharest 77208, Romania.

- (1) (a) Benelli, C.; Gatteschi, D. *Chem. Rev.* **2002**, *102*, 2369–2387, and references therein. (b) Kahn, O. *Acc. Chem. Res.* **2000**, *33*, 647–657. (c) Sakamoto, M.; Manseki, K.; Okawa, H. *Coord. Chem. Rev.* **2001**, *379*, 219–221, and references therein.
- (2) (a) Bencini, A.; Benelli, C.; Caneschi, A.; Carlin, R. L.; Dei, A.; Gatteschi, D. *J. Am. Chem. Soc.* **1985**, *107*, 8128–8136. (b) Bencini, A.; Benelli, C.; Caneschi, A.; Dei, A.; Gatteschi, D. *Inorg. Chem.* **1986**, *25*, 572–575.

- (3) (a) Figuerola, A.; Diaz, C.; Ribas, J.; Tangoulis, V.; Sangregorio, C.; Gatteschi, D.; Maestro, M.; Mahia, J. *Inorg. Chem.* **2003**, *42*, 5274–5281. (b) Sakamoto, M.; Hashimura, M.; Matsuki, K.; Matsumoto, N.; Inoue, K.; Okawa, H. *Bull. Chem. Soc. Jpn.* **1991**, *64*, 3639–3641. (c) Blake, A. J.; Milne, P. E. Y.; Thornton, P.; Winpenny, R. E. P. *Angew. Chem., Int. Ed. Engl.* **1991**, *30*, 1139–1141. (d) Costes, J.-P.; Dahan, F.; Dupuis, A.; Laurent, J.-P. *Inorg. Chem.* **1997**, *36*, 3429–3433, 4284–4286. (e) Stemmler, A. J.; Kampf, J. W.; Kirk, M.; L.; Atasi, B. H.; Pecoraro, V. L. *Inorg. Chem.* **1999**, *38*, 2807–2817. (f) Kahn, M. L.; Sutter, J. P.; Golhen, S.; Guionneau, P.; Ouahab, L.; Kahn, O.; Chasseau, D. *J. Am. Chem. Soc.* **2000**, *122*, 3413–3421.
- (4) (a) Costes, J.-P.; Dahan, F.; Dupuis, A.; Laurent, J.-P. *Inorg. Chem.* **2000**, *39*, 169–173. (b) Costes, J.-P.; Dahan, F.; Dupuis, A. *Inorg. Chem.* **2000**, *39*, 5994–6000.

the 6s orbital of Gd and delocalization tails of the 3d orbital of Cu on the ligand. An alternate explanation by Kahn,⁶ inspired by general schemes due to Goodenough,⁷ proposed a configuration interaction activity of states produced by the one-electron jump between the 3d of the metal ion and the 5d vacant AOs of the lanthanide ion. Kahn's mechanism was based on Extended Hückel estimations, which cannot, however, offer a proper account for the subtle configuration interaction problems. In fact, Kahn expressed a reservation owing to the crudity of the Extended Hückel approach.

Other theoretical studies on the topic are scarce, the phenomenon being incompletely understood. To the best of our knowledge, only one computation⁸ and one general modeling⁹ paper have been devoted to this problem. As briefly discussed below, these works offer a somewhat limited perspective. Thus, in a DFT (ADF) study, Yan and Chen⁸ reported a good reproduction of the J coupling constant for a copper–gadolinium complex. The work also produced spin density maps and Mulliken-type population analysis, leading to an interpretation of the magnetic coupling as a spin delocalization from the copper center and a spin polarization from the gadolinium center. As Benelli and Gatteschi observed in their recent review,^{1a} the mentioned work⁸ gave no discussion about the role of 6s vs 5d polarization mechanisms. A definite problem appears to be that the authors relied on a report on a compound cited from a proceedings¹⁰ claiming a ferromagnetic nature ($J_{\text{exp}} = +2.9 \text{ cm}^{-1}$ vs. $J_{\text{calcd}} = +3.6 \text{ cm}^{-1}$), while the paper containing experimental data for the same compound¹¹ reported a very weak antiferromagnetic coupling $J_{\text{exp}} = -0.039 \text{ cm}^{-1}$. The problem obviously needs reconsideration. The reproduction of small and sensitive values using a method like DFT is prone to nonsystematic tendencies, and its accuracy is then a very delicate problem. In this case, the focus should be kept not on the reproduction of values themselves but on data that are more definitely stable with respect to the method of computation. We appreciate that the ligand spin polarization picture in the discussed work represents valuable progress and it remains robustly valid, independent of the quality of the computed J parameter.

The general success of DFT in connection with Broken Symmetry (BS)¹² strategy as a practical way toward the estimation of coupling constants is illustrated indisputably in state-of-the-art contemporary results.¹³ In d -transition metal ion complexes, the magnetic orbitals originate as a matter of course from frontier MOs of DFT calculations. In contrast, in d -

complexes, the magnetic orbitals of lanthanide subsystems are located deeper than MOs of the d -type and of ligand origins. This makes the handling of the Broken Symmetry scheme (and of the electronic structure calculation itself) rather a delicate problem that should be carefully defined and debated. However, special features of the ADF package¹⁴ (namely the preliminary fragment definition of the input and the option to impose non-*aufbau* occupation numbers) might allow such a specific handling, but the authors did not supply the necessary particulars.

In a recent work,⁹ an intentionally comprehensive many-body Hamiltonian modeling was used. However, despite its rather complex formalisms, this study was based on inappropriate, and in certain respects unreasonable, assumptions. Namely, it was considered that by using zero-differential overlap (ZDO) and Hubbard-type Hamiltonian parametrization, the f shell could be treated with a single pair of Coulomb and exchange integrals. Such an assumption should not be applied to the f shell, where due to symmetry resulting from the 7-fold degeneracy, the two-electron integrals cannot be equated simply by Hubbard-like Hamiltonians (which are generally valid for interactions between different centers with one orbital per site). It is true that the f two-electron integrals can be expressed in terms of a finite set of Slater radial parameters (F^k , $k = 0, 2, 4, 6$) and the number of free parameters can be empirically reduced by assuming certain ratios between the F^k , as practiced sometimes in lanthanide spectroscopy.¹⁵ However, the authors of the mentioned study⁹ did not make any specific reference to using integrals in accordance with F^k proper parametrization and appropriate symmetry coefficients.

The magnetochemistry of the past decade has evolved as an example of symbiotic evolution between theory and experiment. The chemistry of binuclear or oligonuclear exchange-coupled metal ions has offered simpler and clearer case studies for understanding this interaction. In turn, the theoretical advances have offered fruitful and clear rules of thumb for introducing rational synthetic approaches to systems with ferromagnetic coupling. Groups working in this field often combine the chemical and theoretical language. On the other hand, the chemist's interest in theory is generally confined to qualitative levels. In view of this, a proper theoretical certification of the revealing concepts circulating in the field is needed. As an example of the ongoing question of the ferromagnetic coupling in Cu(II)–Gd(III) systems, we will quote from the conclusion of a recent paper:¹⁶ "...results point out the need for more experimental/theoretical studies about this heterometallic system in order to get a clear answer". This phenomenon has already had substantial experimental development,^{1–6} while its theoretical aspects are still schematic,^{8,9} thus indicating that new quantum chemical investigations would be an indispensable development. The present work undertakes this task, covering

- (5) (a) Benelli, C.; Caneschi, A.; Gatteschi, D.; Guillou, O.; Pardi, L. *Inorg. Chem.* **1990**, *29*, 1750–1755. (b) Benelli, C.; Caneschi, A.; Fabretti, A. C.; Gatteschi, D.; Pardi, L. *Inorg. Chem.* **1990**, *29*, 4153–4155.
 (6) (a) Kahn, O. *Struct. Bonding* **1987**, *68*, 89–167. (b) Kahn, O. *Angew. Chem., Int. Ed. Engl.* **1985**, *24*, 834–850. (c) Ramade, I.; Kahn, O.; Jeannin, Y.; Robert, F. *Inorg. Chem.* **1997**, *36*, 930–936. (d) Kahn, O. *Molecular Magnetism*; VCH Publishers: New York, 1993. (e) Andruh, M.; Ramade, I.; Codjovi, E.; Guillou, O.; Kahn, O.; Trombe, J. C. *J. Am. Chem. Soc.* **1993**, *115*, 1822–1829. (f) Guillou, O.; Oushoorn, R. L.; Kahn, O.; Boubekeur, K.; Batail, P. *Angew. Chem., Int. Ed. Engl.* **1992**, *31*, 626–628.
 (7) Goodenough, J. B. *Magnetism and the Chemical Bond*; Interscience: New York, 1963.
 (8) Yan, F.; Chen, Z. D. *J. Phys. Chem. A* **2000**, *104*, 6295–6300.
 (9) Rudra, I.; Raghun, C.; Ramasesha, S. *Phys. Rev. B* **2002**, *65*, 224411-1-9.
 (10) Gao, S.; Borgmeier, O.; Lueken, H. *The Third International Conference of Elements Abstract Book*; Porcher, P., Hölsä, J., Eds.; Paris, Sept. 1997.
 (11) Gao, S.; Borgmeier, O.; Leuken, H. *Acta Phys. Polonica A* **1996**, *90*, 393–398.
 (12) (a) Noodleman, L. *J. Chem. Phys.* **1981**, *74*, 5737–5743. (b) Noodleman, L.; Case, D. A.; Aizman, A. *J. Am. Chem. Soc.* **1988**, *110*, 1001–1005. (c) Noodleman, L. *Inorg. Chem.* **1991**, *30*, 246–256.

- (13) (a) Ruiz, E.; Alemany, P.; Alvarez, S.; Cano, J. *J. Am. Chem. Soc.* **1997**, *119*, 1297–1303. (b) Ruiz, E.; Cano, J.; Alvarez, S.; Alemany, P. *J. Am. Chem. Soc.* **1998**, *120*, 11 122–11 129. (c) Gillon, B.; Mathoniere, C.; Ruiz, E.; Alvarez, S.; Cousson, A.; Rajendiran, T. M.; Kahn, O. *J. Am. Chem. Soc.* **2002**, *124*, 14 433–14 441. (d) Ruiz, E.; Cano, J.; Alvarez, S.; Caneschi, A.; Gatteschi, D. *J. Am. Chem. Soc.* **2003**, *125*, 6791–6794.
 (14) Amsterdam Density Functional (ADF) package, see: (a) Boerrigter, P. M.; te Velde, G.; Baerends, E. J. *Int. J. Quantum Chem.* **1988**, *33*, 87–113. (b) te Velde, G.; Baerends, E. J. *J. Comput. Phys.* **1992**, *99*, 84–98.
 (15) Newman, D. J.; Ng, B. K. C. *Crystal Field Handbook*; Cambridge University Press: Cambridge, 2000.
 (16) Ryazanov, M.; Nikiforov, V.; Lloret, F.; Julve, M.; Kuzmina, N.; Gleizes, A. *Inorg. Chem.* **2002**, *41*, 1816–1823.

new and rather comprehensive details and solving the mechanism of general Cu(II)–Gd(III) ferromagnetic coupling.

II. Results and Discussion

1. Computational Details and Methodology. We employed different computational packages, exploiting their complementary options. Thus, MOLCAS-5¹⁷ was used for CASSCF, CASCI, CASPT2¹⁸ and MS-CASPT2¹⁹ calculations with ab initio model potentials (AIMP)²⁰ and GAMESS²¹ was employed for schemes using the effective core potentials (ECP), effective fragment potentials (EFP)²² and CASSCF with localized orbitals. The experimental system comprising the study case is discussed later, with mention of the reasons for its conversion to a symmetry-idealized prototype.

The idealized molecule was produced by optimizing the [CuL–Lu] complex at the ROHF level, using Lu³⁺ in order to avoid the problems raised by an open shell for lanthanide ions. In this way, a reasonable geometry of the ligand skeleton in the complex was obtained. The geometry optimization was perfected at the CASPT2 level for the whole [CuL–Gd] complex, by varying only the positions of Cu(II) and Gd(III) ions along the C₂ axis; i.e., the most significant coordinates of the system.

Owing to its novelty, certain technical details will be offered for the DK3-AIMP scheme.²³ The AIMP can be presented as conceptually superior to ECP, whereas for the given problem, both methods can account for the observed phenomenon. The most frequently used quantum mechanical method in the chemistry of heavy elements is the relativistic effective core potential (RECP) approximation.²⁴ In this approximation, the core electrons are modeled using a suitable function, and only the valence electrons are treated explicitly. Some of the relativistic effects, especially the scalar ones, are taken into account without having to perform full 4-component relativistic calculations. The AIMP method has been developed as an extension of the RECP method, and it describes the correct behavior for the inner nodal structure of the valence orbitals. The AIMP model consists of a Coulomb potential, an exchange potential, and a projection operator, and has a clear physical meaning in that it represents the Coulomb and exchange

interactions between a single valence electron and the core electrons. Most recently, the DK3-AIMP-based approach combined with the multistate, complete active space, multiconfigurational second-order perturbation method and a restricted active space state interaction spin–orbit method (MS-CASPT2/RASSI-SO)²⁵ in conjunction with the Douglas-Kroll type of atomic mean-field spin–orbit integrals (DK-AMFI-SO)²⁶ was successfully used in the calculation of the ground and low-lying states of lanthanide and actinide molecules.²⁷ In the present work, we have employed DK3-AIMP and CG-AIMP²⁸ for Gd and Cu atoms in the atomic and molecular calculations. Spin–orbit effects have been included through the DK3-AIMP based MS-CASPT2/RASSI-SO method in conjunction with DK-AMFI-SO integrals. For H, C, N, and O, the 6-31G basis sets have been employed. The calculation were partly repeated considering the 6-31+G* basis set on N and O, certifying that the results are only slightly dependent on such basis set change. The richer basis sets are prohibitive for the full account up to CASPT2 level, whereas the rather moderate ones are enabling reasonable insight for chemically realistic systems, making possible the selection of significantly rich orbital active spaces for investigation of the configuration interactions that are driving the mechanism.

It should be noted that, although the energy scale of the investigated effect is very small (a few cm⁻¹), it is well accounted for in all the mentioned computation schemes. Disregarding the small numerical differences between various techniques, this illustrates the relative robustness of the interaction mechanism. We maintained a focus on detailed interpretation of the output from the various numerical experiments, rather than insisting on good numerical reproduction of experimental data or making conclusions about the hierarchy of performance of the different computation methods and codes.

2. Choice of a Prototypical System; The Non-aufbau Structure of the *d–f* Transition Metal-Lanthanide Complexes. To gain insight into the topic with the assistance of quantum mechanical calculations, we have selected a prototypical molecule from the chemical work of Costes et al.²⁹ This system is representative of the large series of Cu–Gd and other *d–f* related complexes. It has a binucleating (compartmental) structure, with a quasi-square planar coordination of the *d*-transition metal ion, ensuring a larger coordination place, that is made with oxygen donor moieties, which is able to accommodate the voluminous lanthanide ion. The lanthanide coordination at this site is completed by outer counterions. The main structural features of the adopted [CuL–Gd] prototype are close to those of many *d–f* transition metal complexes.^{30,31}

The CASSCF calculation on the experimental molecule (including the semicoordinated NO₃⁻) gave a 30.7 cm⁻¹

- (17) Andersson, K.; Barysz, M.; Bernhardsson, A.; Blomberg, M. R. A.; Cooper, D. L.; Fülscher, M. P.; Graaf, C. de; Hess, B. A.; Karlström, G.; Lindh, R.; Malmqvist, P.-Å.; Nakajima, T.; Neogrády, P.; Olsen, J.; Roos, B. O.; Schimmelpfennig, B.; Schütz, M.; Seijo, L.; Serrano-Andrés, L.; Siegbahn, P. E. M.; Ståhring, J.; Thorsteinsson, T.; Velyazov, V.; Widmark P.-O. MOLCAS Version 5.4. Department of Theor. Chem., Chem. Center, University of Lund, P.O. Box 124, S-221 00 Lund, Sweden, Lund, 2002.
- (18) Andersson, K.; Malmqvist, P.-Å.; Roos, B. O. *J. Chem. Phys.* **1992**, *96*, 1218–1226. Andersson, K.; Malmqvist, P.-Å.; Roos, B. O.; Sadlej, A. J.; Wolinski, K. *J. Phys. Chem.* **1990**, *94*, 5483–5488.
- (19) Finley, J.; Malmqvist, P.-Å.; Roos, B. O.; Serrano-Andrés, L. *Chem. Phys. Lett.* **1998**, *288*, 299–306.
- (20) Huzinaga, S.; Seijo, L.; Barandiarán, Z.; Klobukowski, M. *J. Chem. Phys.* **1987**, *86*, 2132–2145. Seijo, L.; Barandiarán, Z.; Huzinaga, S. *J. Chem. Phys.* **1989**, *91*, 7011–7017.
- (21) Schmidt, M. W.; Baldridge, K. K.; Boatz, J. A.; Elbert, S. T.; Gordon, M. S.; Jensen, J. H.; Koseki, S.; Matsunaga, N.; Nguyen, K. A.; Su, S. J.; Windus, T. L.; Dupuis, M.; Montgomery, J. A. *J. Comput. Chem.* **1993**, *14*, 1347–1363.
- (22) (a) Day, P. N.; Jensen, J. H.; Gordon, M. S.; Webb, S. P.; Stevens, W. J.; Krauss, M.; Garmer, D.; Basch, H.; Cohen, D. *J. Chem. Phys.* **1996**, *105*, 1968–1986. (b) Jensen, J. H. *J. Chem. Phys.* **2001**, *114*, 8775–8783.
- (23) (a) Paulović, J.; Nakajima, T.; Hirao, K.; Seijo, L. *J. Chem. Phys.* **2002**, *117*, 3597–3604. (b) Tsuchiya, T.; Nakajima, T.; Hirao, K.; Seijo, L. *Chem. Phys. Lett.* **2002**, *361*, 334–340.
- (24) (a) Phillips, J. C.; Kleinman, L. *Phys. Rev.* **1959**, *116*, 287–294. (b) Huzinaga, S.; Cantu, A. A. *J. Chem. Phys.* **1971**, *55*, 5543. (c) Bonifacic, V.; Huzinaga, S. *J. Chem. Phys.* **1974**, *60*, 2779–2786. (d) Katsuki, S.; Huzinaga, S. *Chem. Phys. Lett.* **1988**, *152*, 203–206. (e) Sakai, Y.; Miyoshi, E.; Klobukowski, M.; Huzinaga, S. *J. Comput. Chem.* **1987**, *8*, 226–255.

- (25) Malmqvist, P.-Å.; Roos, B. O.; Schimmelpfennig, B. *Chem. Phys. Lett.* **2002**, *357*, 230–240.
- (26) Marian, Ch. M.; Wahlgren, U.; *Chem. Phys. Lett.* **1996**, *251*, 357–364.
- (27) (a) Diaz-Megias, S.; Seijo, L.; *Chem. Phys. Lett.* **1999**, *299*, 613–622. (b) Paulović, J.; Nakajima, T.; Hirao, K.; Lindh, R.; Malmqvist, P.-Å. *J. Chem. Phys.* **2003**, *119*, 798–805.
- (28) Barandiarán, Z.; Seijo, L. *Can. J. Chem.* **1992**, *70*, 409–415.
- (29) Costes, J.-P.; Dahan, F.; Dupuis, A.; Laurent, J.-P. *Inorg. Chem.* **1996**, *35*, 2400.
- (30) (a) Gleizes, A.; Julve, M.; Kuzmina, N.; Alikhanyan, A.; Lloret, F.; Malkerova, I.; Sanz, J. L.; Senoçq, F. *Eur. J. Inorg. Chem.* **1998**, *1169*, 9–1174. (b) Sasaki, M.; Manseki, K.; Horiuchi, H.; Kumagai, M.; Sakamoto, M.; Sakiyama, H.; Nishida, Y.; Sakai, M.; Sadaoka, Y.; Ohba, M.; Okawa, H. *J. Chem. Soc., Dalton Trans.* **2000**, 259–263. (c) Brianese, N.; Casellato, U.; Tamburini, S.; Tomasin, P.; Vigato, P. A. *Inorg. Chim. Acta* **1999**, *293*, 178–194.

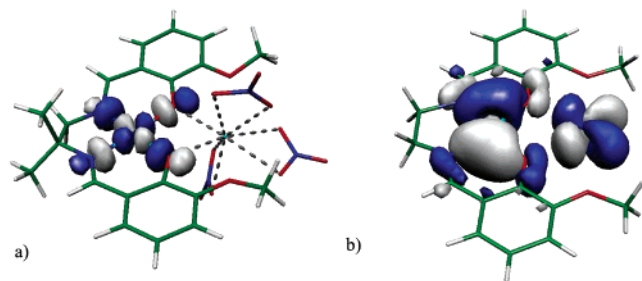


Figure 1. Quasi- C_{2v} symmetry of orbital shapes in Cu–Ln complexes with binucleating ligands. (a) The natural orbital resulting from CASSCF(8,14) calculations on the experimentally observed structure of the molecule considered to be a structural prototype. The departure from true C_{2v} symmetry comes from asymmetric ligand substitution and the placement of semi-coordinated NO_3^- counterions. (b) The orbital density difference map for the orbital centered on [CuL] (the optimized CASSCF MO of the [CuL-Gd] complex, minus the ROHF MO of the separate [CuL] entity). The change was genuinely small and is magnified here by using a $0.002 \text{ e}/\text{\AA}^3$ contour value.

ferromagnetic gap, extremely close to the experimental value²⁹ of $4J_{\text{exp}} = 28 \text{ cm}^{-1}$. Even with such a perfect reproduction of the coupling strength at hand, we treat the ab initio calculation not as a way to retrieve experimental data but as a source of correct balance between various parameters that drive the phenomenon. Therefore, in the subsequent work we proceeded with a series of considerations and computational experiments targeting this goal.

The above-mentioned study molecule has a general skeleton (and especially a coordination moiety) close to C_{2v} symmetry, while it does not possess true symmetry elements. However, the peripheral substitution, or the slight distortions from the overall planarity of the molecule, do not impinge upon the effective C_{2v} nature of the environment of the metal ion couple. The CASSCF natural orbital assignable to the [CuL] part of the system (with experimental geometry) is located, as predicted by ligand field theory, in the plane of the $\{\text{N}_2\text{O}_2\}$ donor set and has virtually a C_{2v} -like shape (see Figure 1a).

The accumulated experimental data allowed certain magneto-structural correlations in terms of an exponential-type dependence of coupling strength on the Cu...Gd distance³² and as a function of CuO_2Gd dihedral angle in butterfly-type bending.^{6c,33a} While the distance-type correlation is not generally well held, the observation that the deviation from planarity of the [CuL–Gd] skeleton reduces the ferromagnetic gap offers a good qualitative rule of thumb for defining the quasi-planarity of the metal ions–ligand frame as a decisive structural factor.^{33b} Here, we have made use of this finding. The importance of the pseudo- C_{2v} symmetry actually parallels the observed experimental correlation of ferromagnetism with the planarity of the $\text{CuO}_2\text{–Gd}$ fragment.

Given the above considerations, the starting experimental structure was further idealized (by geometry optimization) to

C_{2v} symmetry, to get a better insight into the mechanism. This study molecule is then not a real one, but it is realistic. The symmetry designation throughout this paper is with regard to the z -axis along the Cu–Gd pair, and the ligand is placed in the yz plane. The ground exchange split state configurations then have ${}^9\text{B}_1$ and ${}^7\text{B}_1$ designations.

The calculations on d – f systems represent a special problem due to the non-*aufbau* structure of the d – f transition metal–lanthanide complexes. Thus, the f^7 form an inner shell. The unpaired electron of the [CuL] complex is the HOMO orbital. In the [CuL–Gd] complex, it may keep this character, but it is separated from the other α electrons (located on gadolinium) by a large gap, containing many double occupied orbitals of [CuL]. Therefore, a regular self-consistent procedure (based on single determinant with *aufbau* configuration) is not working. This is probably the reason for the lack of ab initio calculations on Cu–Gd systems in the existing literature. However, this technical difficulty can be understood and treated appropriately by considering the physics of the system.

The red-line of our approach can be summarized briefly: starting CASSCF and CASPT2 computations with fragment based wave functions, to design the correct insertion of the f shell in the whole MO diagram; obtaining a good ab initio account of the ferromagnetic gap (by direct calculation); designing a comprehensive analytical model of the Gd(III) and for the coupling mechanism, feeding it with parameters extracted from thorough analysis of the ab initio data; investigating the role of the ligand and ligand field by means of various computational experiments (the discrimination of various orbital and CI interaction channels determining the ferromagnetic coupling); and elaborating conclusions illuminating the qualitative views of the well-known experimental magneto-structural correlation represented by the intrinsic Cu–Gd ferromagnetism, understanding also factors causing the few antiferromagnetic exceptions.

3. Electron Density Distribution and the Exchange Mechanism; Reasons for Spin Polarization Models. A revealing picture of the interaction is gained from working with the density difference map for the orbital shapes belonging to the [CuL] fragment, as was initially introduced in the CI calculations, and those optimized by the CASSCF procedure. This is given in Figure 1b, noting that the effect is strongly magnified here, for better visibility, using rather small contour value: $0.002 \text{ e}/\text{\AA}^3$. Therefore, the effect does not represent a large density flow. The artificial magnifying of a small orbital change serves to show that it consists of: (i) practically no change in d -content of the transition metal center as at this site the density flow is merely p -shaped; (ii) ligand polarization expressed as a sign alternation along the bridge from Cu(II) to Gd(III); and (iii) acquisition of d -character on the lanthanide center as a suggestion of effectiveness of d -type transfer interaction; moreover, note that the d -like density difference recorded on Gd(III) shows asymmetric lobes, which implies d – f hybridization.

The aspects in note (iii) are seen at a “real scale” in the small Gd tails of the b_2^{CuL} CASPT2 orbital in Figure 3, which is also similar to the CASSCF orbital employed here.

Another illustrative computational experiment was done within an active space constructed with symmetrized Pipek–Mezey localized orbitals. The active space included the doubly occupied b_2 functions located on the bridging oxygen atoms,

- (31) (a) Kahn, O.; Pei, Y.; Verdager, M.; Renard, J. P.; Sletten, J. *J. Am. Chem. Soc.* **1988**, *110*, 782–789. (b) Georges, R.; Kahn, O.; Guillou, O. *Phys. Rev. B* **1994**, *49*, 3235–3242. (c) Guillou, O.; Bergerat, P.; Kahn, O.; Bakalbassis, E.; Boubekeur, K.; Batail, P.; Guillot, M. *Inorg. Chem.* **1992**, *31*, 110–114. (d) Evangelisti, M.; Bartolome, F.; Bartolome, J.; Kahn, M. L.; Kahn, O. *J. Magn. Magn. Mater.* **1999**, *197*, 584–585. (e) Kahn, M. L.; Verelst, M.; Lecante, P.; Mathoniere, C.; Kahn, O. *Eur. J. Inorg. Chem.* **1999**, 527–531.
- (32) Benelli, C.; Blake, A. J.; Milne, P. E. Y.; Rawson, J. M.; Winpenny, R. E. *P. Chem. Eur. J.* **1995**, *1*, 614–618.
- (33) (a) Costes, J.-P.; Dupuis, A.; Laurent, J.-P. *New J. Chem.* **1998**, *22*, 1525–1529. (b) Costes, J.-P.; Dahan, F.; Dupuis, A.; *Inorg. Chem.* **2000**, *39*, 165–168.

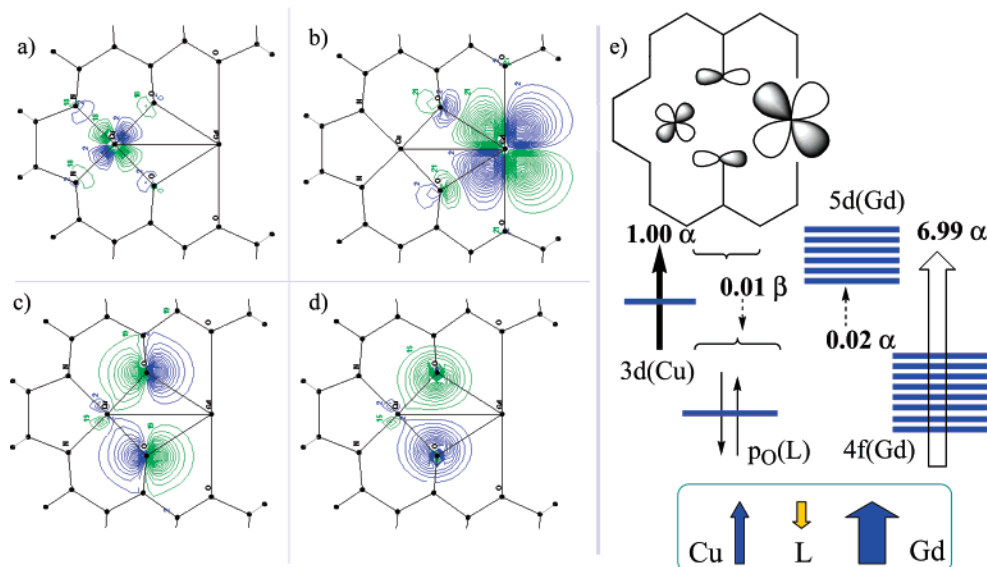


Figure 2. (a)–(d) Selected functions of the CASSCF calculation in the space of symmetry localized orbitals (Pipek-Mezey type); (e) The scheme for slight spin polarization over Cu(II), Gd(III) and the ligand. The orbital depicted in (c) carries almost the complete polarization and delocalization effects, with populations (0.98 α , 0.97 β), whereas those of (d) are practically inert, with (1.00 α , 1.00 β). The small 0.02 α population on the virtual 5d AO of Gd (see b) virtually originates from just one bridge orbital (see c).

apart from the SOMO $d(b_2)$ on Cu and the 4f, 5d, 6s shells of Gd. The CASSCF calculation performed on this selection yielded a 36 cm^{-1} ferromagnetic gap, bigger than those obtained in the standard CASSCF version described below. This provides important information in that the depicted bridging orbitals are the basic route of the exchange phenomenon. The actual computation experiment provided an illustration of the polarization mechanism (see Figure 2). The sum of α and β populations in the selected orbitals (weighted with CASSCF configuration coefficients) show that the ligand group orbital consisting of p -type oxygen orbitals (oriented tangentially to the CuO_2Gd ring) are more involved in the bonding. This orbital is the main source of density flow corresponding to the slight delocalization toward the virtual orbitals of gadolinium. Its spin densities for α and β are 0.97 and 0.98, respectively, while the other ligand b_2 orbital remained close to perfect double occupancy. The SOMOs of the ground configuration are all close to 1.00 α population. Rounding the numbers to two digits, this shows a slight polarization mechanism with 0.01 β resultant on the bridge localized orbital while the copper center keeps to almost 1.00 α , and the densities summed on gadolinium f and d orbitals are 6.99 α and 0.02 α , respectively. The main contributor among the virtual orbitals is the 5d AO with b_2 symmetry. Therefore, the polarization mechanism involves the 5d AO on gadolinium rather than the 6s (with a_1 symmetry), as was initially supposed in the early qualitative proposals of Gatteschi.⁵

4. Specifics of Electron Configuration of Gd(III) Ion; Toward a Comprehensive Analytical Scheme of Ferromagnetic Coupling Mechanism. A determining structural aspect that is conserved in various (chemically different) ligand surroundings is obviously the ionic character of Gd(III), with the f^7 configuration contracted inside the atom (i.e., a core-like character). Despite being a different sort of problem, the same characteristics determine the ferromagnetism of metallic gadolinium.³⁴ Gadolinium, either as an atom or ion, is a key element in several problems related to ferromagnetic coupling.

Table 1. Analytical Formulas of the $^8\text{S} \rightarrow ^6\Gamma$, Transition Energies for the f^7 Configuration and Corresponding Numeric Data of Gd(III)

	CASSCF SBKJC	CASPT2 AIMP	RCI (ref 38)	exp (ref 39)
$F^2 = 225F_2$	530.20	560.71	544.02	504.90
$F^4 = 1089F_4$	68.88	61.02	90.11	46.63
$F^6 = 184041F_6/25$	7.34	7.08	4.00	5.76
^6P $15 F^2 + 165 F^4 + 3003 F^6$	41350	39732	37683	32580
^6I $35 F^2 + 189 F^4 + 1715 F^6$	44158	43295	39436	36371
^6D $41 F^2 + 297 F^4 + 1001 F^6$	49540	48197	44807	40321
^6G $90 F^2 + 101 F^4 + 1638 F^6$	66693		54584	
^6F $70 F^2 + 231 F^4 + 2002 F^6$	67714		59726	
^6H $85 F^2 + 249 F^4 + 1729 F^6$	74904		97105	

Therefore, we focused on the description of electronic states of the Gd(III) ion. The ^8S ground state has essentially an f^7 character. A small admixture with other states is due to the spin–orbit coupling. This causes the so-called zero-field splitting (ZFS) of the ^8S state. The computation within the AIMP-CASPT2 setting gave here 0.2 cm^{-1} for the total ZFS splitting on Gd(III), which is in full agreement with the experimental data.³⁵ The spin sextet states 6L belong to quantum numbers $L = 1$ to 6. It is interesting to note that, all the $^6L(f^7)$ spectral terms have different orbital quantum numbers and therefore do not interact with each other if the spin–orbit terms are at first ignored. Moreover, the excitations to empty d and s shells are acting in higher orders. The single excitations to f^6d or f^6s are not mixing with the ground or first excited states because of different parity when compared with the f^7 parentage. The Gd(III) ion can therefore be regarded as almost free of electron correlation which, aside from the degeneracy effects, is making the spectroscopy of lanthanide systems a delicate topic.³⁶

(34) Maiti, K.; Malagoli, M. C.; Magnano, E.; Dallmeyer, A.; Carbone, C. *Phys. Rev. Lett.* **2001**, *86*, 2846–2849.

(35) (a) Borel, A.; Yerly, F.; Helm, L.; Merbach, A. E. *J. Am. Chem. Soc.* **2002**, *124*, 2042–2048 (b) Smirnova, T. I.; Smirnov, A. I.; Belford, R. L.; Clarkson, R. B. *J. Am. Chem. Soc.* **1998**, *120*, 5060–5072. (c) Powell, D. H.; NiDubhghaill, O. M.; Pubanz, D.; Helm, L.; Lebedev, Y. S.; Schlaepfer, W.; Merbach, A. E. *J. Am. Chem. Soc.* **1996**, *118*, 9333–9346. (d) Sharma, R. R. *Phys. Rev. B.* **1984**, *30*, 1178–1181.

Using the well-known Slater parametrization of the two-electron integrals, analytical formulas can be obtained for the f^7 spectral terms (see Table 1 and Supporting Information). For the case of two-shell configurations, denoted with subscripts a and b , the traditional Slater–Condon notations of independent radial integrals, which act as parameters in any general two-electron integrals are as follows

$$F_k^{ab} = \int \int R_a(1)^2 \frac{r_{<}^k}{r_{>}^{k+1}} R_b(2)^2 dr_1 dr_2 \quad (1)$$

and

$$G_k^{ab} = \int \int R_a(1) R_b(1) \frac{r_{<}^k}{r_{>}^{k+1}} R_a(2) R_b(2) dr_1 dr_2 \quad (2)$$

For one-shell problem, the F_k integrals are coinciding with the G_k ones. In total, there are 13 parameters describing Coulomb and exchange interactions within and between d and f shells. The complete account for $f+d+s$ gives rise to 24 radial parameters.³⁷

It is acknowledged that the ab initio accounts overestimate the values of parameters, a reduction factor of about 0.8 in F_k integrals being usually acceptable for amendment of the results.³⁸ In Table 1 the F_2 , F_4 , and F_6 parameters obtained from several calculations are given comparatively to those fitted from experimental data³⁹ (Gd(III) embedded in LaCl₃). For gadolinium, almost all standard calculations (ECP or AIMP based CASSCF and CASPT2) overestimate the transition energies, clearly due to overestimation of the F_k integrals as determined by the basis set quality, while the intricate correlation effects can be partly ruled out for the reasons given above.

The $f-d$ parametrization and the corresponding atomic calculations are numerically available within the program package developed by Cowan.⁴⁰ Here we performed analytical derivations of the corresponding integrals and of the CI matrix elements. The analytical handling was performed by our programs, with the help of the computer package Mathematica.⁴¹ In a section below, we use F_k and G_k parameter sets as a suggestive characterization of the gadolinium ion in the molecule.

With the help of analytical formulas for spectral terms and integrals on gadolinium, and fitted here to the “ion-in-molecule” status (see next section), the model of inter-center transfer can be revisited in detail, equating explicitly all the Hamiltonian components. Let us consider a simple two state-model with

$$\Psi_0(S) \equiv \Omega(2^{S+1} B_1 \{^2 B_2 [Cu^{II}(^2D)] \otimes ^2 A_2 [Gd^{III}(^8S)]\}) \quad (3)$$

corresponding to the antisymmetrized product of localized ion

ground-state configurations (d^9 and f^7) and the excited configuration

$$\Psi_1(S) \equiv \Omega(2^{S+1} B_1 [Gd^{II}(2^{S+1}D)]) \equiv \hat{a}_+(d_{Gd}) \hat{a}_-(d_{Cu}) \Psi_0(S) \quad (4)$$

created by the one-electron jump from the [CuL] side to the empty $5d$ orbital of gadolinium (with b_2 representation). Both configurations, their diagonal energies and off-diagonal term, can be ascribed as generally dependent on the spin S , by means of corresponding factors containing the spin coupling operator $\hat{S}_{Cu} \cdot \hat{S}_{Gd}$ as follows

$$E_0(S) = \langle \Psi_0(S) | \hat{H} | \Psi_0(S) \rangle = -J_0 \hat{S}_{Cu} \cdot \hat{S}_{Gd} \quad (5)$$

$$E_1(S) = \langle \Psi_1(S) | \hat{H} | \Psi_1(S) \rangle = \Delta E_{01} - \frac{9}{4} g_{fd} \hat{S}_{Cu} \cdot \hat{S}_{Gd} \quad (6)$$

$$H_{01}(S) = \langle \Psi_0(S) | \hat{H} | \Psi_1(S) \rangle = f_{01} - \frac{9}{4} J_{01} \hat{S}_{Cu} \cdot \hat{S}_{Gd} \quad (7)$$

where

$$\Delta E_{01} = h(d_{Gd}) - h(d_{[CuL]}) - g_{df} + 7F_0^{df} - C_0 + \frac{9}{4} J_0 \quad (8)$$

is the spin averaged gap between configurations, with C_0 and J_0 as Coulomb and exchange parts, and the intra atomic $5d-4f$ interaction is comprised in

$$g_{df} = \frac{1}{4} \left(\frac{3}{5} G_1^{df} + \frac{4}{15} G_3^{df} + \frac{10}{33} G_5^{df} \right) \quad (9)$$

The f_{01} is the spin averaged Fock-time matrix element between the above-defined states, whereas l_{01} is related to its exchange part. The second-order perturbation applied to the above quantities with respect of $\hat{S}_{Cu} \cdot \hat{S}_{Gd}$ part yields the coupling constant J of the effective Heisenberg–Dirac-van Vleck spin Hamiltonian

$$J \approx J_0 + \frac{9}{4} \frac{g_{df} f_{01}^2}{\Delta E_{01}^2} - \frac{9}{2} \frac{f_{01} l_{01}}{\Delta E_{01}} \quad (10)$$

In all the above formulas orthogonalized orbitals were tacitly employed. As mentioned in following, the overlap between [CuL] and Gd orbitals was proved negligibly small by the direct analysis of the ab initio integrals. All the parameters in the above formulas were fitted from the ab initio integrals extracted from a GAMESS²¹ run with the SBKJC-ECP definition for gadolinium.

5. Systematic Check of Interaction Pathways. An insight into the coupling mechanism is gained from calculations on the hypothetical “naked” pair Cu(II)–Gd(III), located at the same distance as in the complex. As seen in Table 2, this already yields a very small ferromagnetic coupling. Subsequently, part of the ligand effects were added with the help of effective fragment potential (EFP)²² techniques. This method is usually designed for combined quantum-molecular mechanics (QM–MM) calculations and solvent effects. As an aside, we note that these techniques are also suited to include effects assignable to the basic ideas of ligand field theory. Namely, within EFP, a

(36) (a) Morrison, C. A.; Leavitt, R. P. In *Handbook on the Chemistry and Physics of Rare Earths*; Gschneider, K. A., Ed.; North-Holland: Amsterdam, 1982. (b) Edvardsson, S.; Aberg, D.; *Computer Physics Communications* **2001**, *133*, 396–406.

(37) In the $R_k^{[a,b][c,d]}$ notation, the generalized parameters are as follows: $R_0^{[s,s][s,s]}$, $R_1^{[s,d][s,s]}$, $R_2^{[s,d][s,d]}$, $R_3^{[d,d][s,s]}$, $R_4^{[d,d][s,d]}$, $R_5^{[d,d][d,d]}$, $R_6^{[d,d][d,d]}$, $R_7^{[s,f][s,f]}$, $R_8^{[d,f][s,f]}$, $R_9^{[d,f][d,f]}$, $R_{10}^{[d,f][d,f]}$, $R_{11}^{[d,f][d,f]}$, $R_{12}^{[d,f][d,f]}$, $R_{13}^{[d,f][d,f]}$, $R_{14}^{[d,f][d,f]}$, $R_{15}^{[d,f][d,f]}$, $R_{16}^{[f,f][s,s]}$, $R_{17}^{[f,f][s,d]}$, $R_{18}^{[f,f][s,d]}$, $R_{19}^{[f,f][d,d]}$, $R_{20}^{[f,f][d,d]}$, $R_{21}^{[f,f][d,d]}$, $R_{22}^{[f,f][f,f]}$, $R_{23}^{[f,f][f,f]}$, $R_{24}^{[f,f][f,f]}$, $R_{25}^{[f,f][f,f]}$.

(38) Dzuba, V. A.; Sushkov, O. P.; Johnson W. R.; Safronova, U. I. *Phys. Rev. A* **2002**, *66*, 032105-1-6.

(39) Kielkopf, J. F.; Crosswhite, H. M. *J. Opt. Soc. Am.* **1970**, *60*, 347.

(40) (a) Cowan, R. D. *The Theory of Atomic Structure and Spectra*; University of California Press: Berkeley, 1981. (b) Cowan codes are available at ftp://aphysics.lanl.gov/pub/cowan/ or http://www.t4.lanl.gov.

(41) Wolfram, S. *Mathematica*, Version 4 for Windows; Cambridge University Press: Cambridge, 1999.

Table 2. Illustrative Quantities for Cu–Gd Systems: Computed Ferromagnetic Gap, Its One- and Two-electron Parts, and Fit of Gd-Type Slater–Condon Radial Parameters to the Computed Set of Molecular Integrals^a

system	Cu(II)–Gd(III) "naked" dimer	Cu(II)–Gd(III) in "pure" ligand field (EFP).	[CuL–Gd]	[CuL–Gd]	[CuL–Gd]
method	CI, CASSCF	CI, CASSCF	CI-only	CI-only	CASSCF
active space	$d_{\text{Cu}}+(f^7sd^5)_{\text{Gd}}$	$d_{\text{Cu}}+(f^7sd^5)_{\text{Gd}}$	$d_{\text{Cu}}+(f^7)_{\text{Gd}}$	$d_{\text{CuL}}+(f^7sd^5)_{\text{Gd}}$	$d_{\text{CuL}}+(f^7sd^5)_{\text{Gd}}$
$\Delta E_{\text{ferro}} = 4J$	0.02	0.30	0.40	2.95	12.02
one-electron energy	+0.22	+5.07	−0.83	+37.03	+72.67
two-electron energy	−0.20	−4.77	+1.23	−34.08	−60.645
F_0^{dd}	89066.3	89069.6		89917.4	86814.4
F_2^{dd}	47855.9	47855.9		48441.1	47761.5
F_4^{dd}	31400.7	31400.8		31935.7	31360.7
F_0^{df}	111612.5	111616		112498.9	114267.9
F_2^{df}	27759.2	27759.2		28244.9	27816.8
F_4^{df}	13377.8	13377.8		13666.4	13473.2
G_1^{df}	21581.3	21581.5		22037.6	21434.9
G_3^{df}	12467.4	12467.4		12743.2	12507.6
G_5^{df}	8563.0	8562.9		8752.6	8620.8
F_0^{ff}	249152.5	249152.4	249170.3	249170.3	247947.6
F_2^{ff}	119296.1	119296.2	119314.3	119314.3	120000.1
F_4^{ff}	75010.9	75011.20	75023.0	75023.0	72629.4
F_6^{ff}	54010.0	54010.30	54022.1	54022.1	55067.1
$R_{\text{non zero}}^{\text{abs } b}$	0	0.08	0.78	9.62	132.09
$R_{\text{non zero}}^{\text{rel}}$	0	0.04	0.0005	0.007	0.05
$R_{\text{zero}}^{\text{abs}}$	0	0.27	2.40	3.18	12.05

^a All energy quantities are expressed in cm^{-1} . ^b The molecular series includes the role of the ligand in a progressive manner. The $R_{\text{non zero}}^{\text{abs}}$ is the absolute mean deviation for the Gd integrals that are nonzero in the spherical ion, and $R_{\text{non zero}}^{\text{rel}}$ is the corresponding relative quantity. The $R_{\text{zero}}^{\text{abs}}$ is the deviation from the symmetry vanishing atomic integrals, being a measure of the aspheric deformation in the coordinated ion.

fragment, which in our case is the negatively charged binucleating ligand, can be prepared (at the expense of a separate RHF run) as being represented by a collection of multipole effects (from point charges up to octopoles). The Cu(II)–Gd(III) ion pair was placed in the field of such electrostatic and polarization effects. As lanthanide ion is practically in pure ionic form and the transition metal experiences a weak covalence (partly ionic) regime, the EFP treatment includes a substantial component of the effects exerted by the ligand environment toward the metal ions. Obviously, by this means, no orbital overlap effects are included. The Cu(II)–Gd(III) pair exposed to the pure ligand field exerted by the organic fragments shows only a slight increase in ferromagnetic splitting, demonstrating that certain overlap factors cause physically detectable coupling.

The following step consisted of the addition of a metal–ligand interaction in a nonvariational manner. For this purpose, an MO basis set was created by joining the HF eigenvectors from a separate [CuL] unit with those of free Gd(III). This construction follows on from the fact that the f electrons are expected to be well isolated in their shell, with weak interaction capabilities. The merged orbital set had very small, practically negligible, LCAO values in the off-diagonal ([CuL], [Gd]) blocks. There was a deviation from zero which allowed the orthogonalization necessary to use the CI routine. The overlap between [CuL] MOs and Gd(III) AOs is very small, the maximum value being 0.008; it is created from the empty d orbital of the lanthanide placed in the ligand plane and having lobes oriented toward bridge (b_2). The overlap with the f functions of the same symmetry is about 0.0003.

A CI performed on a basis consisting of the b_2 d -type orbital from the [CuL] fragment and $f+d+s$ shells of gadolinium (all orbitals kept frozen) gives a firm amount of 2.95 cm^{-1} , i.e., a

rather significant ferromagnetic gap. However, if under the same conditions, the active space includes only the orbitals carrying the unpaired electrons, namely the d -type MO on [CuL] plus the f^7 set on gadolinium, the gap remains small at 0.4 cm^{-1} . This indicates the importance of the interaction related to the electron transfer from copper to empty d orbitals of the lanthanide ion. The separation between the ground-state nonet and the septet increases if the CI is considered variationally, via CASSCF calculations. The ordering of computed coupling strength as a function of the selected computational setting (see Table 2) allows us to understand part of the phenomenon; namely, that the ligand plays an active role, while the naked dimer or those undergoing only ligand field effects show only a small coupling magnitude. The CASSCF performed over active the $d_{\text{CuL}}+(f^7s)_{\text{Gd}}$ limited active space gave the 0.39 cm^{-1} splitting, suggesting that the polarization via $6s$ shell of gadolinium is rather limited.

The role of empty d orbitals is also determined, according to the results of active space tuning. However, under any circumstances, one may state also that the ferromagnetic effect is intrinsic to the Cu(II)–Gd(III) pair and exists, at small splitting values, even in the absence of CI contributors that are enhancing the coupling.

By extracting the effective single-electron integrals (the Fock matrix elements with respect to the closed configuration of the core orbitals) and all the two-electron integrals, together with the corresponding cofactors in the monoparticle and biparticle density matrices, the total gap can be dichotomized as shown in the second and third data lines of Table 2. Even though the terms that are due basically to direct exchange integrals have positive values, the total balance of various nonexchange, general type integrals running in the density matrix formula of

the energy is acting against the ferromagnetic effect. The effect is restored owing to the one-electron component, where, notably, the leading terms are related to changes on the diagonal elements of the [CuL] 3*d*-type orbital and also on a weakly populated 5*d* Gd AO with the same symmetry (*b*₂), as well on their off-diagonal matrix elements. This tells us that the mechanism of inter-center electron hopping between *d*-type orbitals can be described as the channel effective for ferromagnetic coupling. This result is also compatible with an interpretation as a ligand polarization effect.

A progressive step was to consider all of the two-electron integrals attributable to the Gd(III) component and to fit them in terms of full analytical formulas discussed above. This is a nontrivial task and it helps to reveal useful information from the rich data contained in the black box of the ab initio calculations. The various *F_k* and *G_k* parameters are given in Table 2. The relatively small variation of the intrinsic Gd(III) parameters along the sequence of computational schemes proves its ionic status. The small alterations suggest a slight nephelauxetic effect. A certain ion asymmetry is induced owing to the bonding effects, illustrated by increased deviation from spherical parametrization at the CASSCF stage. This deformation may have a significant impact on the mechanism of exchange coupling, allowing the potential interplay of *f* → *d* excitations on Gd(III), which were forbidden by spherical symmetry.

The parameters employed in formulas 5–10 were computed with the ab initio integrals extracted from the system obtained with merged SCF wave functions of separate [CuL] and Gd(III) (the orthogonalization of small overlaps between fragment MOs was also performed). This system is considered as an appropriate sample on which to judge the basic sources of interaction, starting from isolated magnetic orbitals, avoiding the complex effects due to small delocalization tails appearing in the variational wave functions. In this case, the replacement of corresponding parameters⁴² shows that the inter-center *d*–*d* jump modeled in this way accounts for only approximately 20% of the ferromagnetic gap computed for the same system at the CI level. This suggests that, with respect to purely unperturbed fragment states, the Kahn's mechanism may not be the unique contributor to the overall ferromagnetic coupling constant. Alternate CI sources were identified in the excited states that resulted from local 4*f* → 5*d* excitations inside of lanthanide. Such orbital promotions are helping the lanthanide ion to acquire the diffusiveness necessary to interact with the copper center. Note that single excitations between *f* and *d* shells that are forbidden by parity in the free gadolinium ion become allowed by symmetry in the C_{2v} environment of the complex.

One has to point out that the above modeling overestimates the *E*₁, *E*₀ energies owing to the lack of static correlation considered in the computational experiment (i.e., the CI on unperturbed fragment configurations). The refinement by CASPT2 (as discussed later) gives a smaller magnitude, around 120 000 cm⁻¹. In this case, the Kahn mechanism becomes preponderant to the exchange gap. However, the choice of the crude computation stage chosen for the above as a basis of parametric

(42) Aside to parameters of Table 2, the following quantities were extracted from ab initio integrals: *J*₀ = 0.05 cm⁻¹, *C*₀ = 225 964.96 cm⁻¹, *h*(*d*_{Gd}) – *h*(*d*_{Cu}) = –342 450.27 cm⁻¹, the energy gap between ground and excited states is 199 804.6 cm⁻¹ when *S* = 4 and 219 077.3 cm⁻¹ when *S* = 3; analogously, *H*₀₁ are –939.5 cm⁻¹ vs. –915.2 cm⁻¹ and *l*₀₁ = 24.4 cm⁻¹.

Table 3. Ferromagnetic Gap at Various CASSCF and CASPT2 Calculations Based on AIMP Basis Sets for Metal Ions^a

active space	1	2	3	4	5	6
on [Cu ^{II} L]	<i>d</i> (<i>b</i> ₂)	<i>d</i> (<i>b</i> ₂)	<i>d</i> (<i>b</i> ₂)	<i>d</i> ⁵	L ⁸ <i>d</i> ⁵	L ²⁰ <i>d</i> ⁵
on Gd ^{III}	<i>f</i> ¹ <i>sd</i> ⁵	<i>f</i> ¹ <i>sd</i> ⁵	<i>f</i> ¹ <i>sd</i> ⁵	<i>f</i> ¹ <i>sd</i> ⁵	<i>f</i> ¹ <i>sd</i> ⁵	<i>f</i> ¹ <i>sd</i> ⁵
no. of electrons	8	8	8	16	32	56
method	AIMP non relativistic ^b	[CuL] frozen	[CuL] relaxed	CI-only	CI-only	CI-only
CASSCF	10.73	11.27	11.31	12.53	20.56	21.51
CASPT2	10.42	11.25	>30			

^a All energy values are in cm⁻¹. ^b All the calculations, except for the denoted column, are including by default the relativistic part of AIMP.

interpretation is justified by the fact that the merged fragment type wave functions are particularly close to the idea of magnetic orbitals as states especially localized on metal ions, expressing the status of the system “in advance” of interaction.

6. Multi-State Studies within Complete Active Space and Second-Order Perturbation Techniques. Here, we introduce the first CASPT2 studies of the topic, done with MOLCAS code, within AIMP description of metal ions. The CASPT2¹⁸ method has gained a reputation as one of the methods with the highest accuracy and efficiency. It is able to compute quantities related to small energy scale effects occurring in the various electronic structure problems of transition metals⁴³ and exchange coupled systems.⁴⁴ Additionally, the method works by constructing an effective Hamiltonian in the framework of second-order perturbation theory. This follows from first principles, the basic ideas of phenomenological molecular magnetism, where the total coupling constant is seen as the sum of direct exchange integrals and various second order terms. The CASPT2 study has the same basic conclusions obtained from different versions of CASSCF calculations. New computational experiments in the topic were designed within this scheme. For instance, detecting rather small changes in the ferromagnetic gap after switching off the relativistic part of the AIMP, we were able to testify that the discussed phenomenon is not essentially due to the relativistic effects (see Table 3) and therefore not strongly influenced by spin–orbit coupling. The CASPT2 orbital pictures (Figure 3) are illustrating the fact that Gd(III) part can be described with almost pure *f* orbitals and the [CuL] part (mainly due to 3*d* of copper) effectively includes a tail containing small fraction of 4*f* and 5*d* AOs of gadolinium.

One must note that in the CASPT2 calculations, the doubly occupied orbitals (RAS1 type) comprised between the unpaired Gd *f*-like functions are located deeper in the energy scheme (see Figure 4a) and the *d*-like functions localized mostly on [CuL] were necessarily kept frozen. The unusual electronic structure, with the active occupied MOs placed between many inactive doubly occupied orbitals, imposed this freezing technique. In the full nonfrozen CASPT2 procedure, the calculations cannot be used quantitatively, owing to imperfect convergence, whereas the tendency to increase the ferromagnetic gap (as

(43) Roos, B. O.; Andersson, K.; Fulscher, M. P.; Malmqvist, P.-Å.; Serrano-Andres, L.; Pierloot, K.; Merchan, M. *Adv. Chem. Phys.* **1996**, *93*, 219–331.

(44) (a) Ceulemans, A.; Heylen, G. A.; Chibotaru, L. F.; Maes, T. L.; Pierloot, K.; Ribbing, C.; Vanquickenborne, L. G. *Inorg. Chim. Acta* **1996**, *251*, 15–27. (b) Ceulemans, A.; Chibotaru, L. F.; Heylen, G. A.; Pierloot, K.; Vanquickenborne, L. G. *Chem. Rev.* **2000**, *100*, 787–806. (c) de Graaf, C.; Sousa, C.; Moreira, I. D.; Illas, F. *J. Phys. Chem. A* **2001**, *105*, 11 371–11 378; (d) Suaud, N.; Bolvin, H.; Daudey J. P. *Inorg. Chem.* **1999**, *38*, 6089–6095.

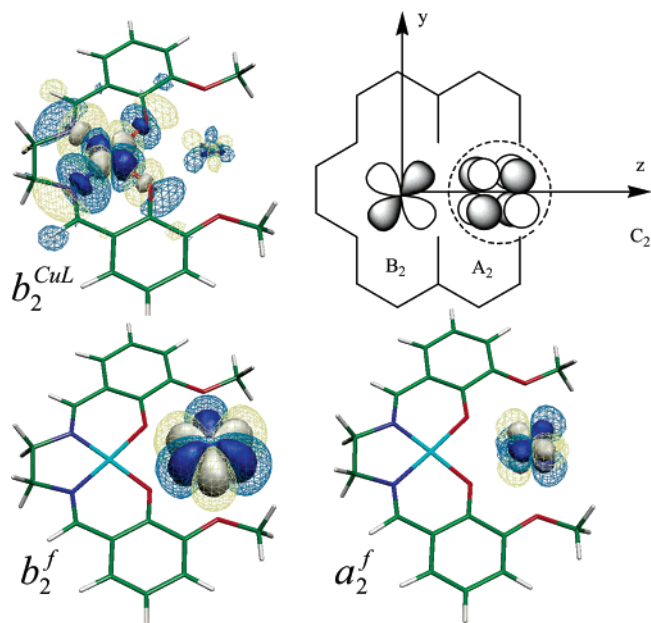


Figure 3. CASPT2 orbitals, which are relevant to the wave functions ascribed in formula (11). The f orbital with a_2 symmetry can be regarded as providing a dominant part of the coupling effect, having an orthogonality relationship with the magnetic orbital on the [CuL] fragment (with b_2 representation).

compared to CASSCF) tells us, qualitatively, that the ligand polarization effects, which are expected to be involved here, play an important role in the magnitude of effective ferromagnetic coupling. A portion of the ligand polarization terms are

taken into account by performing extended CI calculation on the basis of CASSCF orbitals. This CI recovers effects that were neglected owing to the MO freezing in the CASPT2 part. The stepwise enlarging of the active space contributes to the increase of the ferromagnetic gap, toward a plateau value extrapolated to 22 cm^{-1} .

The wave function is an interesting object, having 97–99% of the content of the configuration consisting in almost unmodified fragment orbitals, while as mentioned in the Introduction, the single-determinant HF or DFT calculations are not able to directly produce this result, owing to nonstandard ordering of singly and doubly occupied orbitals. In addition to the main term, there are many others, with small coefficients. Retaining a few components only, the functions are as follows

$$\Psi_{\text{CI}}^{S=4} \text{ and } \Psi_{\text{CASPT2}}^{S=4} = 0.99|(d.o.)(b_2^{\text{CuL}})^\alpha(f^{\text{Gd}})^{7\alpha}| + \dots$$

$$\Psi_{\text{CASPT2}}^{S=3} = (0.95\hat{S}_-(b_2^{\text{CuL}}) + 0.19\hat{S}_-(1b_2^f) - 0.16\hat{S}_-(2b_2^f) + 0.14\hat{S}_-(a_2^f))|(d.o.)(b_2^{\text{CuL}})^\alpha(f^{\text{Gd}})^{7\alpha}| + \dots$$

$$\Psi_{\text{CASPT2}}^{S=3} = (0.98\hat{S}_-(b_2^{\text{CuL}}) + 0.14\hat{S}_-(a_2^f))|(d.o.)(b_2^{\text{CuL}})^\alpha(f^{\text{Gd}})^{7\alpha}| + \dots \quad (11)$$

The low-spin wave function is written with the help of orbital spin lowering operators. The notation $\hat{S}_-(MO)$ suggests that the MO denoted in parentheses undergoes the $\alpha \rightarrow \beta$ switch. It is remarkable that the main part of the $S = 3$ state is due to the spin reversion at the [CuL] b_2 orbital, while showing only small terms corresponding to the spin lowering inside the f shell.

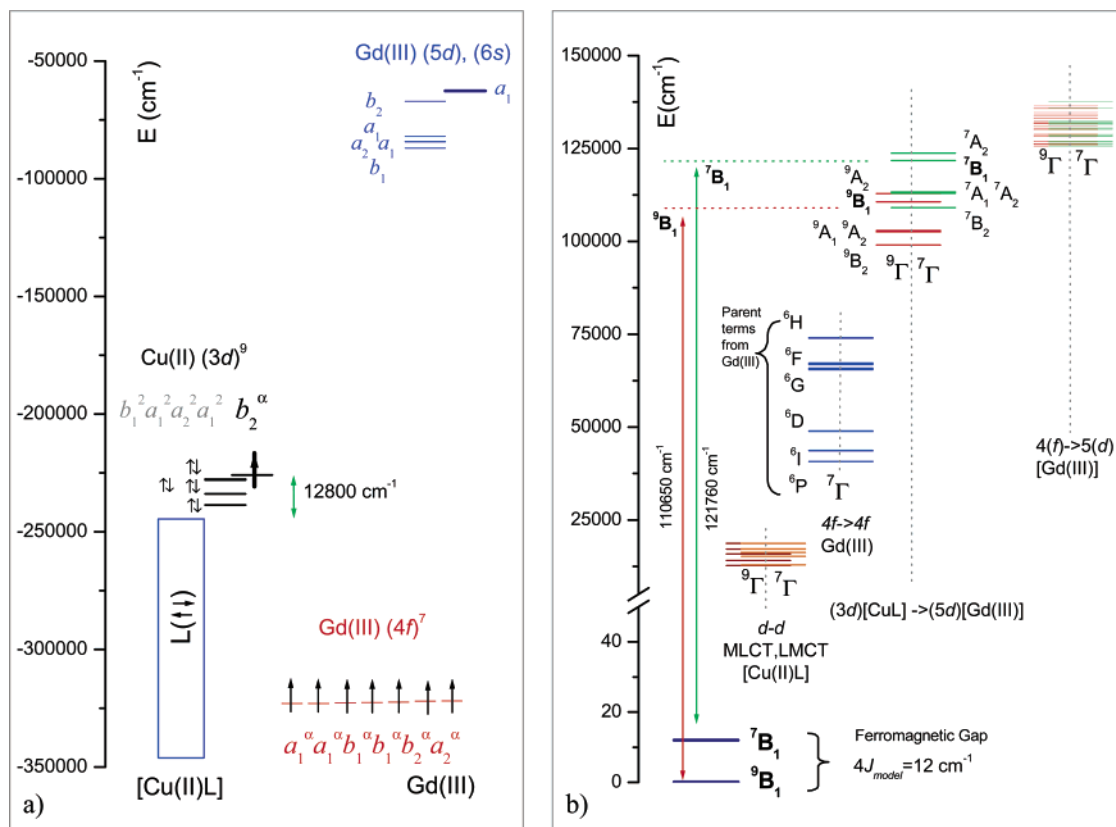


Figure 4. (a) CASPT2 (of G2 type) energies of the active orbitals. The non-*aufbau* structure of the ground state configuration can be seen with the doubly occupied orbitals (d -type and ligand-type of [CuL]) positioned between the $3d$ and $4f$ active orbitals. (b) The excited states of the [CuL–Gd] complex, separated according to their origin. The ligand field transitions on the [CuL] fragment were obtained by extended CI-only calculations. The inter-center $3d-5d$ and Gd-type $4f-5d$ transitions were obtained from MS-CASPT2 over 20 components in each symmetry and spin state.

For the simple CI over the directly merged fragment orbitals, the $\Psi_{\text{CI}}^{S=3}$ show visible β components for the b_2 and a_2 members of the f orbitals. The CAS and PT2 steps are absorbing the b_2^f parts as small Gd-tails in the b_2^{CuL} , letting only the configuration with $(a_2^f)^\beta$ spin-orbital be the most significant among many other small components.

Summing the configuration weights with +1 and -1 for α and β respectively, for each active orbital, the spin coupling on the $S = 3$ state can be condensed as +0.95 and -0.95 populations on a_2^f and b_2^{CuL} respectively, while the other f orbitals are summed to about +0.99 each.⁴⁵ This suggests that the system adopts an effective pathway exchange favoring the orbital orthogonality. The f shell is represented in C_{2v} as $2a_1 + 2b_1 + 2b_2 + a_2$. Formally, the [CuL] exerts overlap only toward b_2 orbitals of the f set, the others being in an orthogonality relationship, corresponding to then to the ferromagnetic pathway. The total coupling can be interpreted as the net preponderance of the number of ferromagnetic pathways (4) as compared to the antiferro pathways (2).

The configuration corresponding to Kahn's mechanism shows quite a low weight. However, one may see that the weight for $S = 4$ is reasonably higher (0.02) than that corresponding to $S = 3$ (0.009). This is in line with the qualitative picture that the ferromagnetic state benefits from an increased portion of this $d-d$ inter-center excitation.

As seen in Figure 4b, the transitions assigned to the inter-center [CuL] to Gd(III) electron jump show a series of related $^9\Gamma$ and $^7\Gamma$ states where the high-spin components of a given orbital symmetry are about 10 000 cm^{-1} lower than the corresponding low-spin case. At the same time, the configurations corresponding to the $f^7 \rightarrow f^6d$ excitations show rather significant weights. This suggests that the differential deformation of Gd(III) in a molecule as a function of spin state is symbiotically contributing to the ferromagnetic coupling. The smaller difference in the weights (0.025 vs 0.019 in $S = 4$ vs $S = 3$) is due to the fact that the series of $^9\Gamma(^8L)$ states (originating from the $L = 1\dots 5$ terms of Gd(III)) are separated from congener $^7\Gamma(^6L)$ ones by a rather small gap (see Figure 4b). Therefore, each term of this type offers a presumably small perturbation stabilization of the high-spin, molecular ground state, while their multitude may be cumulatively significant.

The spin CASPT2 densities weighted for the $S = 3$ state can be presented as $(b_2^{\text{[Cu(II)L]}})^{0.95\beta} (a_2^{\text{[Gd(III)]}})^{0.95\alpha} (a_1^{\text{[Gd(III)]}})^{2\alpha} (b_1^{\text{[Gd(III)]}})^{2\alpha} (b_2^{\text{[Gd(III)]}})^{2\alpha}$. Note that the $a_2(f)$ orbital of Gd(III), with 0.95 α , balances the opposite spin population recorded on the copper center, 0.95 β , whereas the other f orbitals seem less perturbed. Then, the system effectively adopts an orbital orthogonal exchange pathway with b_2 (yz) and a_2 (xyz) symmetries on the [Cu(II)L] and Gd(III) sides. Nevertheless, the overall multi-state picture suggests a rather complex mechanism.

III. Conclusion

Combining all the complementary data offered by various calculation and interpretation schemes, we have arrived at the conclusion that the ferromagnetic gap (between ground $S = 4$ and the next $S = 3$ state) is intrinsic to the Cu(II)–Gd(III) pair. Namely, it appears with a low magnitude ($\sim 0.02 \text{ cm}^{-1}$) for the

naked dimer. The pure ligand field (electrostatic and polarization effects, without covalence) slightly increases the gap (to 0.3 cm^{-1}), while full ab initio treatment including the complete ligand accurately reflects the detectable ferromagnetic gaps (3–36 cm^{-1} , as a function of the settings in the numerical experiments). Using state-of-the-art AIMP's including relativistic effects, we were able to detect by tests that switched out the corresponding terms, that the ferromagnetic coupling is basically not driven by relativistic or spin-orbit effects.

Within an appropriate definition of magnetic orbitals (a good choice being in the CASPT2 framework) the Kahn concept can be certified as an effective mechanism of ferromagnetic coupling. The involved orbitals are not genuine Cu($3d$) and Gd- ($5d$) AOs, but MOs already containing a small tail of Gd-origin on the orbital located mainly on the [CuL] side as well a slight mixing between $4f$ and $5d$ AOs of Gd(III).

We pointed also interesting aspects concerning the Gd(III) ion itself. Namely, due to rather small role of correlation effects in ground and first excited states, the Gd(III) may be regarded as a possible cornerstone for revisiting the model parametrization and ab initio computations in lanthanide spectroscopy.

Appropriate computation experiments (CASSCF over Pipek–Mezey localized orbitals, including the bridging phenolato ones in an active space) gave support to the spin polarization picture, involving the ligand and the $5d$ orbitals of Gd(III). In fact, the CI vs polarization mechanisms of Kahn and Gatteschi, respectively, are not mutually contradictory, but are even interconvertible by appropriate transformations of the magnetic orbitals, thereby adjusting the portion of pure Cu($3d$) and ligand tails, in the active orbital that interacts with Gd($6s$) or Gd($5d$).

The handling of the CASPT2 results shows that the system effectively adopts an orbital orthogonal exchange pathway, the main interaction being concentrated between b_2 [Cu(II)L] and a_2 [Gd(III)] orbitals. Such orbital regularities are held within the C_{2v} symmetry of the molecular prototype. A look at a large series of experimental structures of Cu–Gd ferromagnetic complexes shows that indeed the effective C_{2v} pseudo-symmetry of the coordination frame seems to be generally obeyed. However, in the case of advanced asymmetry, this rule may be broken. Then, the usual configuration interaction forces related to kinetic transfer override the intrinsic ferromagnetic part. Indeed, reported antiferromagnetic exceptions⁴ appear in cases showing asymmetry in the chemical nature of the donor atoms in the ligand. This therefore offers a general qualitative explanation both for the widespread occurrence of the ferromagnetic coupling and for the antiferromagnetic exceptions.

A problem of a slightly different nature, that we chose not to address in the present study, seems to be the magnetic coupling between Gd(III) ions and radical-ligands. While in Cu(II)–Gd(III) complexes only two antiferromagnetic exceptions are known,⁴ for the overwhelming majority of cases recording ferromagnetic behavior^{1–3} in the Gd–radical complexes, both ferromagnetic⁴⁶ and antiferromagnetic⁴⁷ couplings are known. Such aspects may form the targets of new theoretical studies.

A valuable advancement in the present study consisted of pointing out the implications of the non-*aufbau* ground-state

(45) The populations described in this way are those of canonical MOs of CASPT2 calculations and should not be confused with those of natural orbitals or with Mulliken estimations.

(46) (a) Benelli, C.; Caneschi, A.; Gatteschi, D.; Laugier, J.; Rey, P. *Angew. Chem., Int. Ed. Engl.* **1987**, *26*, 913–915. (b) Sutter, J.-P.; Kahn, M. L.; Golhen, S.; Ouahab, L.; Kahn, O. *Chem. Eur. J.* **1998**, *4*, 571–576. (c) Benelli, C.; Caneschi, A.; Gatteschi, D.; Pardi, L.; Rey, P. *Inorg. Chem.* **1990**, *29*, 4223–4228.

configuration for the ab initio approach. A strategy for correct accounting for the implied physical and computational particularities was defined and employed. Such aspects are useful for any calculation involving (*d–f*) hetero-metal ion complexes or lanthanide-radical systems.

Acknowledgment. F.C. gratefully acknowledges the support of JSPS for a postdoctoral fellowship. F.C. and M.F. are indebted to the INTAS foundation (Grant No. 00-00565). J.P. is grateful for a scholarship from the Ministry of Education, Science, Culture, and Sports of Japan under the Japanese

- (47) (a) Lescop, C.; Luneau, D.; Belorizky, E.; Fries, P.; Guillot, M.; Rey, P. *Inorg. Chem.* **1999**, *38*, 5472–5473. (b) Caneschi, A.; Dei, A.; Gatteschi, D.; Sorace, L.; Vostrikova, K. E. *Angew. Chem., Int. Ed.* **2000**, *39*, 246–248. (c) Lescop, Ch.; Belorizky, E.; Luneau, D.; Rey, P. *Inorg. Chem.* **2002**, *41*, 3375–3384.

Government Scholarship Program for Foreign Students. This research was partly supported by a grant-in-aid for Scientific Research in Specially Promoted Research “Simulations and Dynamics for Real Systems”, a Grant for 21st Century COE Program “Human-Friendly Materials based on Chemistry” from the Ministry of Education, Science, Culture, and Sports of Japan, and a grant from the Genesis Research Institute.

Supporting Information Available: Basic molecular information for ab initio calculations and details on analytical formulas in pdf format. This material is available free of charge via the Internet at <http://pubs.acs.org>.

JA030628K